PERFORMANCE OF A COMBUSTION DRIVEN SHOCK TUNNEL

WITH APPLICATION TO THE TAILORED-

INTERFACE OPERATING CONDITIONS

By William J. Loubsky, Robert S. Hiers, and David A. Stewart

NASA, Ames Research Center
Moffett Field, Calif., 94035

ABSTRACT

The performance characteristics of the driven tube portion of a

combustion driven shock tunnel, uniquely designed to give up to several

hundred milliseconds of quasi-steady reservoir conditions, are presented.

These conditions are achieved by controlling the mass flow into the driven

tube with throttling plates employed near the main diaphragm section and

by reducing the initial unsteady expansion strength by using a large

volume driver. The complex wave system established in the driven tube

section is analyzed theoretically for 20 msec using a wave diagram

and two IBM 7094 computer programs which account for real gas effects

and multiple interface-end-wall reflections. The theory is compared

with experimental pressure distributions obtained for a wide range of

initial loading pressures, and for several throttling plates of varying

sonic-orifice area. Shock velocities in the range of 8,000 feet per

second to 15,000 feet per second were obtained experimentally, agreeing

with the computed values to within 3 percent. It is shown experimentally

that total pressure equilibrium in the shock tube can be obtained after

the upstream passage of the reflected shock wave for a wide range of

initial pressure loadings, providing a proper set of throttling plates

is chosen. This condition was also found to be particularly sensitive

to the sonic-orifice area of the plates. Experimental pressure levels in the driven tube were found to be in reasonable agreement with theoretical predictions. The tailored-interface mode of operation was approximately determined within the limitations imposed by the presence of a finite contact surface region.

INTRODUCTION

The testing time in many present day shock-tunnel facilities is limited by large magnitude fluctuations in the pressure of the reservoir gas in the driven tube. This is attributed to the initial unsteady wave system established when the diaphragm is broken. However, a quasi-steady condition can be attained in the reservoir if this initial wave system is sufficiently weakened just after the test-gas reservoir has been established. This "one-cycle shock compression" process is employed in the Ames 1-foot shock tunnel. The design of the facility required a large volume driver section to weaken any unsteady waves propagating into it and a set of throttling plates near the diaphragm station to control the rate of mass flow into the driven tube. By means of these design features it has been possible to obtain quasi-steady reservoir pressures for 100 msec or more.

For some time it has been recognized that none of the wave models commonly used to calculate shock tube performance is entirely adequate for the case with a converging-diverging area discontinuity in the vicinity of the diaphragm section. The present work was undertaken to extend existing methods of calculating shock tube flows for this case and to incorporate recent improvements in theoretical analysis by which

equilibrium real gas results can be obtained for air and other gas
mixtures. An experimental investigation was conducted to test the
validity of this analytical method, as well as to determine the effects
of initial pressure in the driven tube and mass outflow from the driver
section on the pressure history in the test-gas reservoir.

DESCRIPTION OF FACILITY

Design and Operation

The Ames 1-foot combustion driven shock tunnel was designed to
provide up to several hundred milliseconds of quasi-steady reservoir
conditions by employing the "one-cycle shock compression" technique
as reported by Cunningham and Kraus in Reference 1. For present pur-
poses, it is sufficient to state that this condition exists if the fol-
lowing two requirements are satisfied: First, the pressure ratio across
the primary reflected shock wave must approach unity upon entering into
the driver section. Second, the driver-driven tube area ratio must be
sufficiently large, that is, greater than 10, so that the strength of the
upstream traveling unsteady expansion wave, and thus its reflection from
the driver end wall has a negligible influence on the reservoir pressure.
To accomplish these ends, mass flow restricting plates, which serve as
a sonic orifice, are employed between a conical driver-driven tube conver-
gence section and the shock tube diaphragm. This is illustrated in Figure 1,
and in more detail in Figure 2. Furthermore, to operate simultaneously
at the tailored-interface condition (i.e., such that no disturbance is
reflected upon the interaction of the primary reflected shock wave and
the incident contact surface) the sonic-orifice-driven tube area ratio

and the initial driven tube pressure loading are uniquely defined for a particular set of driver conditions. For the present facility the "standard" driver conditions are $P = 340$ atm, $T = 3750°$ R, and $\gamma = 1.60$ resulting from the combustion process of an initial gas mixture of 7.2-percent oxygen, 11.8-percent hydrogen, and 81.0-percent helium (by partial pressure). The mixture is initially loaded at room temperature to a pressure of 51 atm. Figure 1 is a schematic diagram of the shock-tunnel system illustrating the various dimensions.

Instrumentation

For purposes of the present investigation, the driver-driven tube portion of the tunnel (see Figure 1) was instrumented with five pressure transducers, four of which are located in the driven tube. Unbonded-type strain-gage transducers were used to measure pressure histories in the combustion chamber, in the driven tube at a location 5 feet downstream of the diaphragm, and at a dual port located 3.7 feet from the reservoir end wall. A Kistler SLM type-605 quartz-crystal transducer was located in the test-gas reservoir to provide the fast response required to observe the incident and reflected shock pressures and the interactions with the interface. A Kistler SLM type-601 transducer was also located at the dual port mentioned above. Shock velocity was determined using five ionization probes spaced uniformly along the tube.

DRIVEN TUBE PERFORMANCE

Theoretical Analysis

The theoretical performance of shock tubes employing an area change near the diaphragm has been investigated for ideal gases by Russell, Reference 2, and by Alpher and White, Reference 3. Flagg, in Reference 4, developed a detailed perfect gas analysis for defining shock tube tailored conditions. This general approach has been expanded with the use of two IBM 7094 computer programs which account for multiple end wall interface interactions and real gas effects in the test gas.

The first of these programs is dependent upon an assumed one-dimensional mathematical model as illustrated in Figure 3. The assumed wave system and the regions of steady flow conditions are shown on a distance-time diagram and also in a physical schematic diagram for a particular time, t_1. Further assumptions include a perfect gas treatment of the driver gas and negligible viscous effects. Input requirements for the program are the initial conditions prior to diaphragm rupture in regions 1 and 4 and the sonic orifice-driven tube area ratio. The shock tube performance is then determined by a matching of pressure and velocity across the contact surface dividing regions 2 and 3. The program is presently capable of utilizing the real gas properties of air, CO_2, N_2, Ar, and mixtures of CO_2, N_2, and Ar as test gases. Multiple end wall-interface interactions are computed until the reflected wave at this interface is an expansion. At this point the program stops. Information output includes all shock wave and interface velocities and gas properties in regions 1 through 10. The tailored-interface operating condition is

defined when the pressure ratio p_6/p_5 equals unity (i.e., no disturbance is reflected at the incident contact surface). By plotting this ratio versus p_1 from the computer results, the initial driven tube pressure for tailored operation can be determined. For tailoring of the Ames 1-foot shock tunnel, p_1 is shown to equal 0.42 atm for the particular combustion conditions $p_4 = 340$ atm, $T_4 = 3750^\circ$ R, and $\gamma_4 = 1.60$, and sonic orifice-driven tube area ratio of 0.718.

A second IBM 7094 computer program differs from the one just described only with respect to the incident shock velocity. Here the experimental shock velocity of a particular test is part of the information input to the computer. This allows the program to be completely independent of shock tube geometry and thus the resulting gas property output is not dependent on an assumed wave model for generating the incident shock wave. It should be noted that for both programs, the flow is assumed to be isentropic for all regions upstream of the driver-driven gas interface.

The combined results of both programs are used in the following manner. For any single-diaphragm shock tube with or without area change near the diaphragm, an incident shock velocity versus initial driven tube loading pressure curve can be obtained from the first program. This curve is shown in Figure 4, for the present facility, and is the first approximation to the "facility operating line." One test is then made and the resulting point is added to the figure (e.g., point A). Through this experimental point a curve is drawn parallel to the first approximation, which then defines the facility operating line. Without further testing, the second computer program can be employed to obtain the real gas properties for the multiple end wall-interface interactions and driver gas conditions for any desired loading pressure, using now the corresponding shock velocity obtained from

the operating line. A closer estimate of the initial pressure for tailoring is now available, which for the present facility is $p_1 = 0.35$ atm. A tailoring line is defined by connecting the tailored values determined on two or more operating lines. For the range of loading pressures considered in the present paper it is believed that the discrepancy between a facility operating line and its first approximation is due in large part to the wave model assumed for the first program, and to a lesser extent to the effects of viscosity. For the Ames 1-foot shock tunnel this discrepancy is approximately 10 percent. Shock velocities using the above semiempirical procedure for calculating the facility operating line were predicted to within 3 percent during the present series of tests. The average experimental shock velocities are shown in Figure 4 for the various initial pressure loadings. Average values were used here since the velocity was essentially constant along the length of the tube.

The driven tube analysis is extended further by the construction of wave diagrams using the method of characteristics. A representative diagram is shown in Figure 5, where the distance-time history of the wave system extends for 20 msec and includes the important secondary wave interactions. This particular wave diagram was calculated for an initial driven tube pressure of 0.25 atm (the "standard" initial pressure) and for a situation in which the throttling plates were not used. Of particular interest is the phenomenon that exists in the vicinity of the diaphragm (region A). Referring to Figure 2, it is seen that the diaphragm is located 1.50 feet downstream of the large discontinuous area change, the driver-driven tube area ratio being 18.9. When the diaphragm is

ruptured, the upstream traveling expansion creates reflected compression

waves throughout the conical transition section, and is almost entirely

reflected as a compression at the large step discontinuity. This behavior

is illustrated in the pressure-time comparison of Figure 6, where the theo-

retical and experimental pressures are shown for a time of 10 msec after

diaphragm rupture and at a location 5 feet downstream of the diaphragm.

Indicated on the figure are the initial and incident shock-wave pressure

levels. The experimental pressure behind the incident shock wave is not

detectable since the compression waves are being reflected continually

along the finite inlet conical section (again see Figure 2). The resulting

effect of the compressions is to increase the pressure level in the remainder

of the expansion and to accelerate it downstream. Interaction with the

reflected shock wave further accelerates the expansion into the driven

tube reservoir, thereby further compressing the test gas and raising the

reservoir pressure level.

Experimental Results

A test program was carried out in the Ames 1-foot shock tunnel to

verify the theoretical driven tube performance and to observe the effects

of various throttling plate sizes and initial driven tube loading pressures.

One-cycle shock compression results.- Pressure histories were measured

in the reservoir for several hundred milliseconds in order to determine the

effects of various initial pressure loadings on the establishment of the

one-cycle shock compression mode of operation. The resulting data obtained

for initial pressure loadings between 0.014 and 0.816 atm are presented in

Figure 7. It should be noted that for each initial loading the reservoir

pressure is quasi-steady for long times, since no strong shock or expansion

waves are apparent. A pressure cell acceleration is noticeable in all cases. The significant conclusion to be drawn from this figure, however, is that the existence of the one-cycle shock compression mode of operation is nearly independent of the initial driven tube pressure loading for the present inlet configuration.

A series of tests with throttling plates of several different size sonic areas was conducted for an initial driven tube pressure equal to 0.25 atm. Pressure histories in the shock tube reservoir are presented in Figure 8. The pressure histories can be explained physically in terms of the interaction of the shock wave expansion fan system, as reflected from the driven tube end wall (i.e., see Figure 5 for $4 < t < 16$ msec), with the driven tube inlet region. Consider, for example, the case with the sonic orifice-driven tube area ratio = 0.937. A high pressure associated with the reflected shock-expansion wave system is observed. At a later time this entire system is reflected as an expansion from the entrance to the driver (since the pressure in the wave system is higher than that existing in the driver) and returns to the reservoir at about 20 msec. Because the pressure in this system is now lower than that in the combustion chamber, it is reflected from the driver inlet as a compression. This cycle repeats for several hundred milliseconds until final equilibrium is achieved in the tube.

At smaller inlet area ratios the mass-flow rates of driver gas into the driven tube are reduced with the result that the pressure in the initial reflected wave system is lower than that existing in the driver section (e.g., typified by the lowest curve of Figure 8). Hence, this system is reflected as a compression from the driver inlet. This system will, of course, reflect again from the reservoir end of the tube, approach the driver again, and

either be reflected as an expansion or further compression depending on the relative levels of the pressure then existing in the wave system and in the driver.

It is apparent that the pressure is quite sensitive to changes in the sonic area of the throttling plates. In other words, the existence of a one-cycle shock compression depends very strongly on the rate of mass flow into the driven tube.

Tailored interface conditions.- Since one of the motivations for this work was to investigate experimentally the effect of interface tailoring on the resulting characteristics of the entire shock tube, and the reservoir in particular, several tests were made to detect the actual existence of the tailored interface. The results are shown in Figure 9 for initial pressures both above and below those estimated for tailoring. The initial pressures, experimental shock velocity and computer results illustrating multiple shock wave-interface interactions, are shown on the figure. It should be noted that the pressure cell used for these measurements experiences an overshoot and undershoot upon the arrival of the reflected shock wave at all initial pressure loadings, thus making the actual pressure behind the reflected shock wave undetectable. The most likely cause for this phenomenon is an acceleration sensitivity of the cell since care was taken to isolate the gages thermally. For the initial driven tube pressures (lower than required for tailoring) in Figures 9(a) and 9(b) the pressure rises to a quasi-steady level just after the acceleration spike, in accordance with the predicted compression from the computer results. In Figure 9(d) the quasi-steady level is attained through an expansion wave (i.e., for an initial pressure higher than required for tailoring). Instead of the discreet

compression expected from the interaction of a planar shock wave and a nondiffusing planar interface, however, the compression (as well as the expansion) is observed to continually approach the final pressure level. One possible explanation for this phenomenon would be the existence of a diffuse contact region instead of a contact discontinuity. Other factors which could contribute would be the nonplanarity of both the shock wave and the interface due to viscous interactions and imperfect initial diaphragm opening. All three of these mechanisms probably contribute to the observed behavior in varying degrees.

The determination of the tailored interface condition using the semiempirical method discussed previously and illustrated in Figure 4 was shown to require an initial loading pressure = 0.35 atm. The results for this condition are shown in Figure 9(c). Since the pressure is observed to be quasi-steady after the acceleration phenomenon, it is believed that tailoring occurs at this initial pressure. In all cases the experimental results are in good agreement with the theoretical predictions.

Duration of steady flow in the nozzle.- The duration of steady flow in the nozzle has been determined by aerodynamic measurements in the test stream. Free-stream mass-flow rates and stagnation heating rates were measured and normalized to account for the known fluctuations in the quasi-steady reservoir. The period of steady flow conditions in the nozzle was considered to terminate at the time when these normalized quantities departed significantly from an initial constant level. The durations of steady nozzle flow obtained in this fashion from the present study are presented in Figure 10. The experimental time required to establish the quasi-steady

reservoir state (as determined from Figure 9) is also presented in the figure. The time interval between the start of quasi-steady reservoir conditions and the termination of steady nozzle flow approximates the useful flow duration for aerodynamic test purposes. It is observed from Figure 10 that at all the conditions investigated there appears to be substantial test time. In fact, the times are long enough so that the instrumentation techniques originally developed for use at the tailored-interface condition can also be extended to any of the off-tailored conditions investigated.

It should be pointed out that Cunningham in Reference 1 reports a test time of about 180 msec at the tailored-interface condition in this facility. In the present investigation this order of time corresponds to the onset of essentially pure driver gas flow through the nozzle. Small-scale interface mixing and thus the dilution of the test gas is tentatively advanced as the explanation for the relatively short duration or steady nozzle flow obtained in the present study.

CONCLUDING REMARKS

The performance of the shock tube portion of a combustion driven shock tunnel has been investigated for a constant set of driver conditions. The unique design features of the facility are a large volume driver section and several sonic orifice throttling plates, which enable the attainment of several hundred milliseconds of quasi-steady reservoir pressures.

A semiempirical method employing two 7094 computer programs was used to analyze the shock tube performance for approximately 5 msec. The analysis was extended to 20 msec by a theoretical wave diagram which accounts for several secondary wave interactions. When the wave system established in this diagram is observed, wave motion in the driven tube can be predicted at times greater than 20 msec. To verify the above analysis, experimental tests were made for widely varying initial loading pressures in the driven tube and for several sonic orifice-driven tube area ratios. The pressure levels obtained in these tests were in agreement with the results of the computer program and the wave diagram.

It has been experimentally demonstrated that long periods of quasi-steady reservoir pressures can indeed be established over a wide range of initial driven tube pressures. This condition was shown to be strongly dependent on the sonic orifice-driven tube area ratio. The tailored-interface operating condition was approximately determined, within the limitations imposed by the presence of a finite contact surface region.

The duration of steady flow in the shock tunnel nozzle was investigated by measuring several aerodynamic variables. The results indicate that at least several milliseconds of steady nozzle flow can be attained over the range of reservoir conditions of these tests. Experiments are continuing in this facility to determine the usefulness of these reservoir conditions in the simulation of aerodynamic flight environments.

References

1. National Aeronautics and Space Administration TN D-1428 (October 1962);
    A 1-Foot Hypervelocity Shock Tunnel in Which High-Enthalpy Real-Gas Air
    Flows Can Be Generated With Flow Times of About 180 Milliseconds,
    B. E. Cunningham and S. Kraus.

2. Guggenheim Aeronautical Laboratory California Institute of Technology
    Memo No. 57 (July 20, 1960); A Study of Area Change Near the Diaphragm
    of a Shock Tube, D. A. Russell. Army Ordinance Contract No.
    DA-04-495-ORD-1960.

3. General Electric Co. Report 57-RL-1664 (January 1957); Ideal Theory of
    Shock Tubes with Area Change Near Diaphragm, R. A. Alpher and D. R. White.

4. Avco Corporation Research and Development Div. RAD TM-63-64 (September 30,
    1963); Detailed Analysis of Shock Tube Tailored Condition, R. F. Flagg.

FIGURE TITLES

Figure 1.- Schematic drawing of Ames 1-foot shock tunnel.

Figure 2.- Detail of driven tube inlet showing throttling plates and diaphragm arrangement.

Figure 3.- Wave model used by first computer program. (a) Physical location of pressure waves at a time t_1. (b) Distance history of unsteady pressure waves.
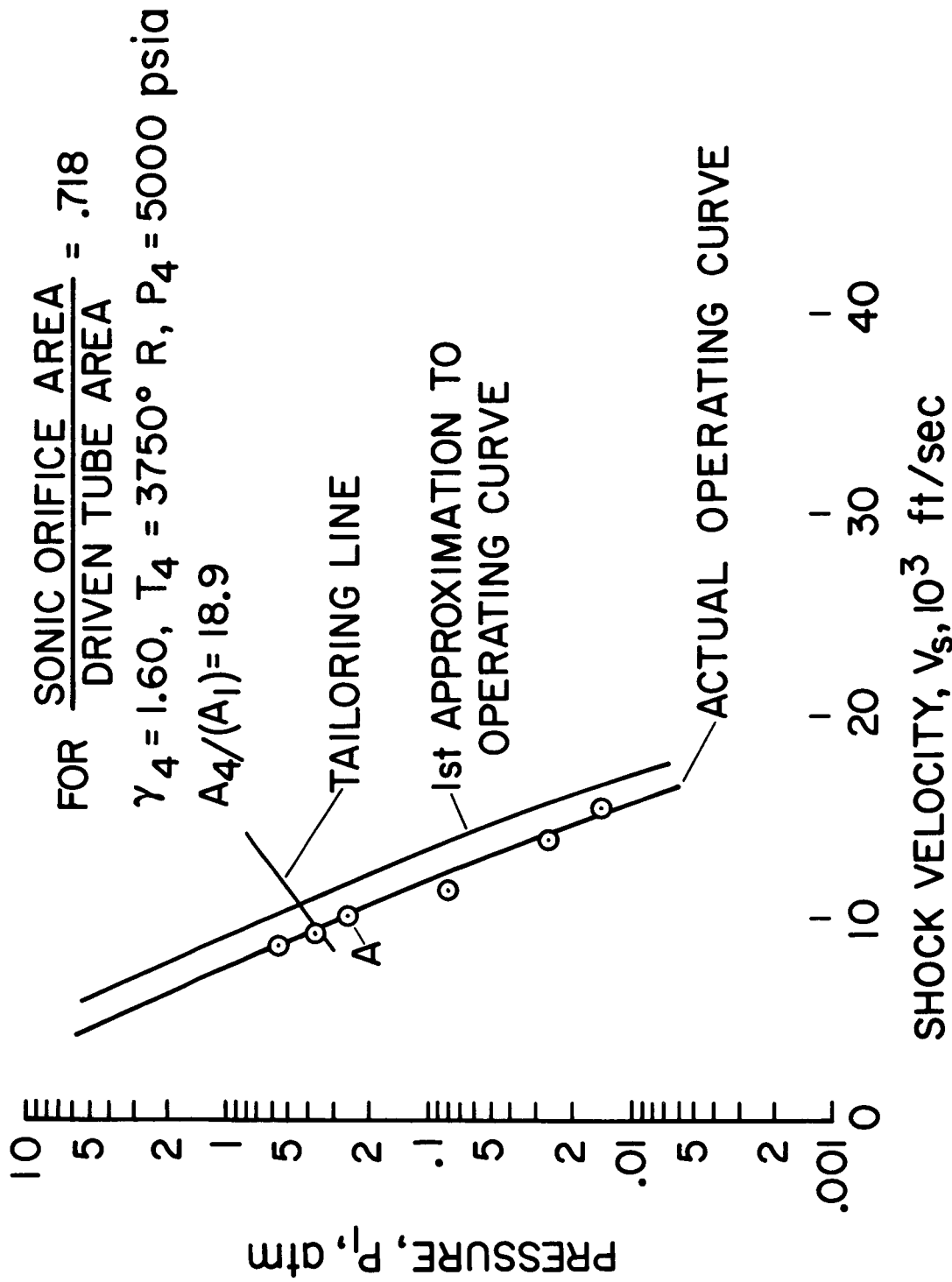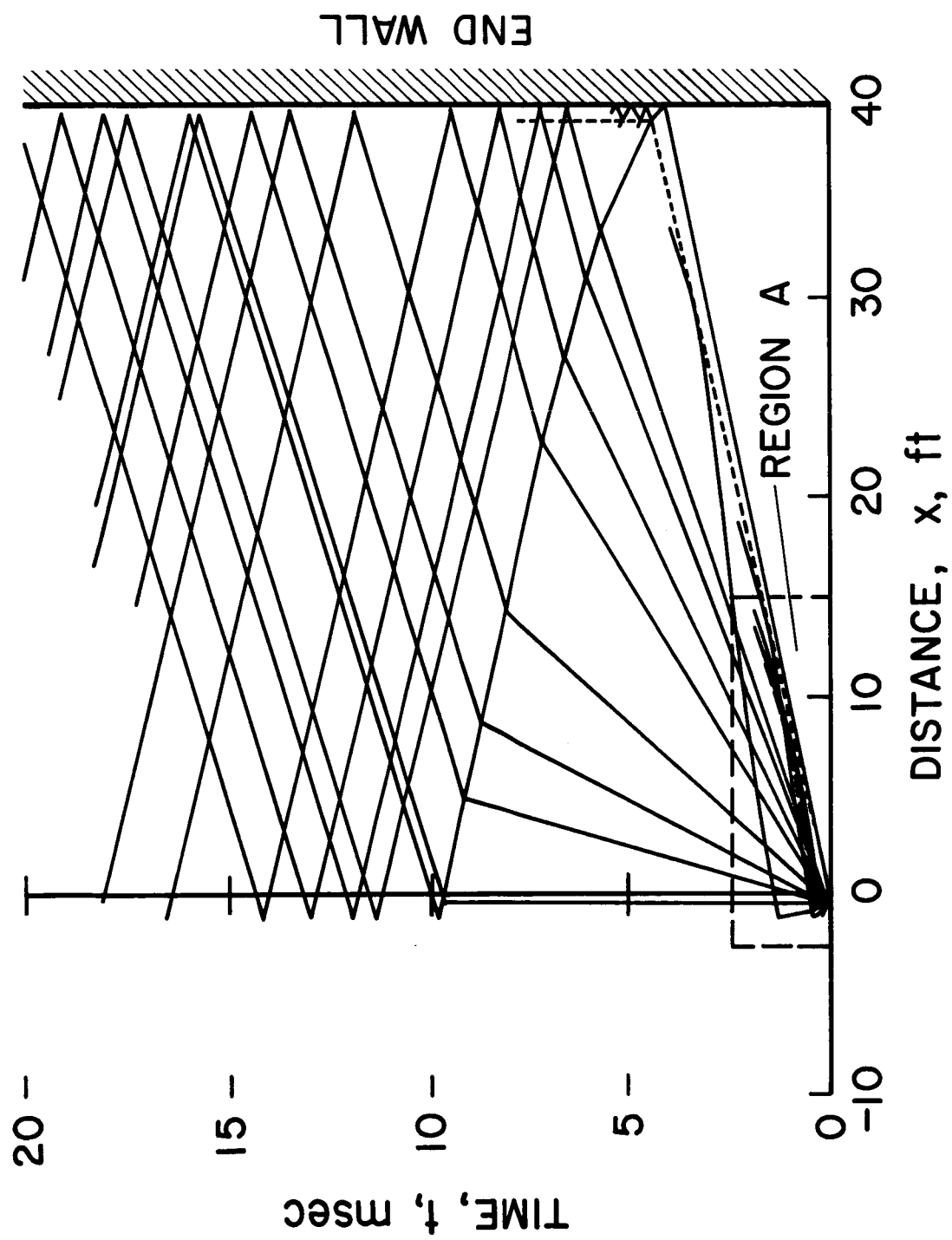
Figure 4.- Facility operating lines.

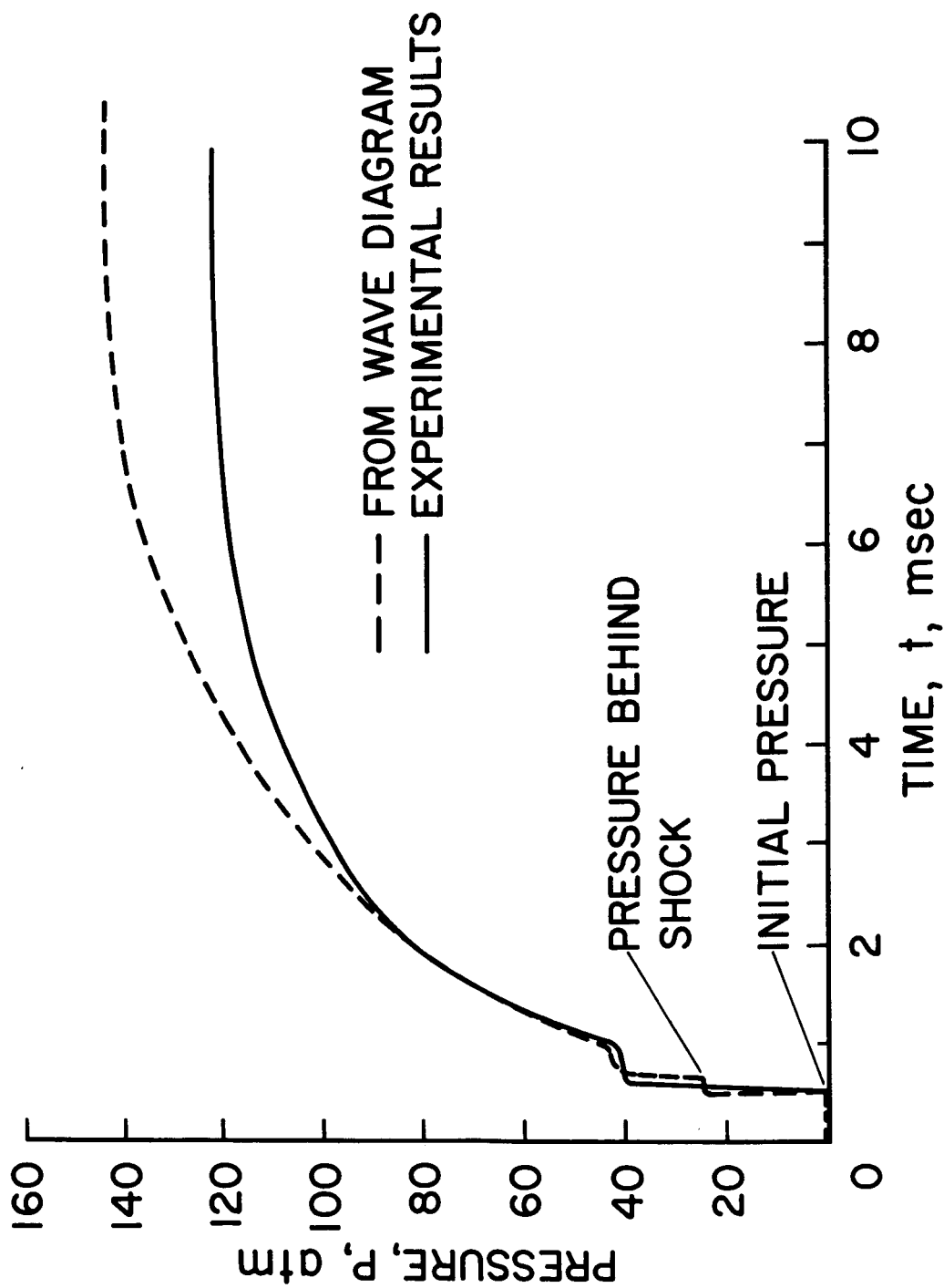Figure 5.- Wave diagram for the driven tube; $P_1 = 0.25$ atm, no throttling plates.

Figure 6.- Comparison between theoretical and experimental pressures obtained at a station 5 feet downstream of the diaphragm.
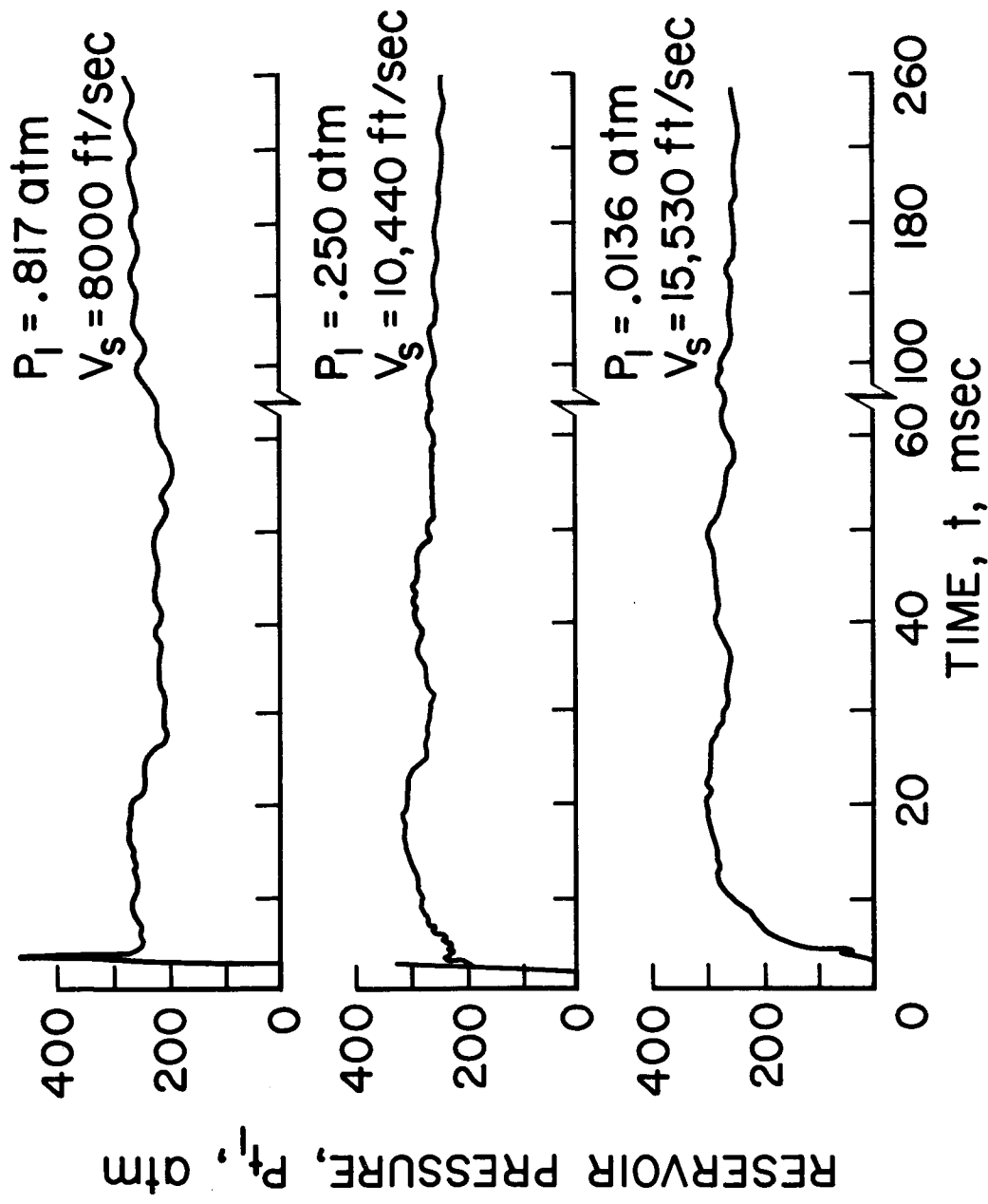
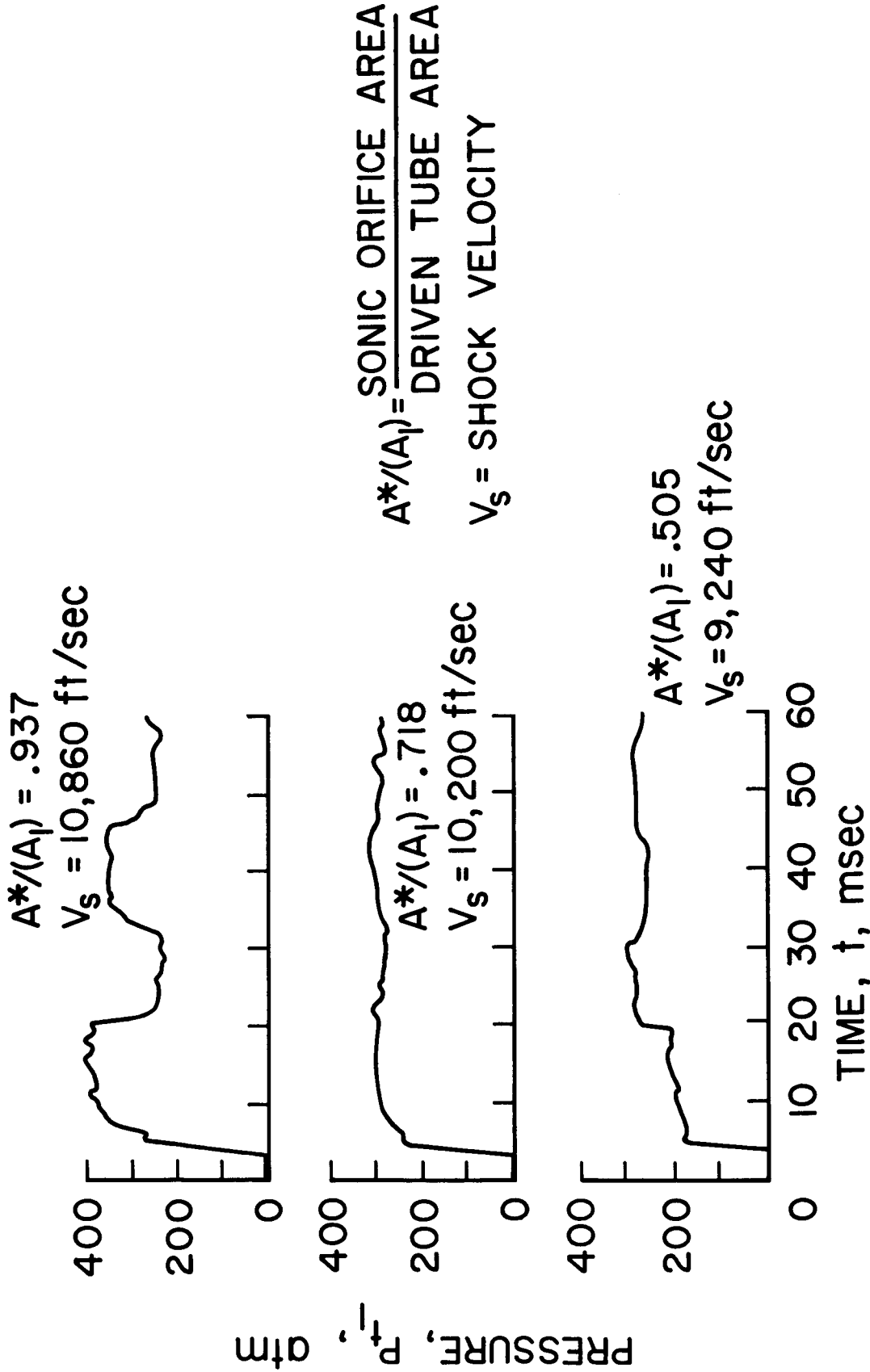Figure 7.- Long-time reservoir pressure history for various driven tube loadings.

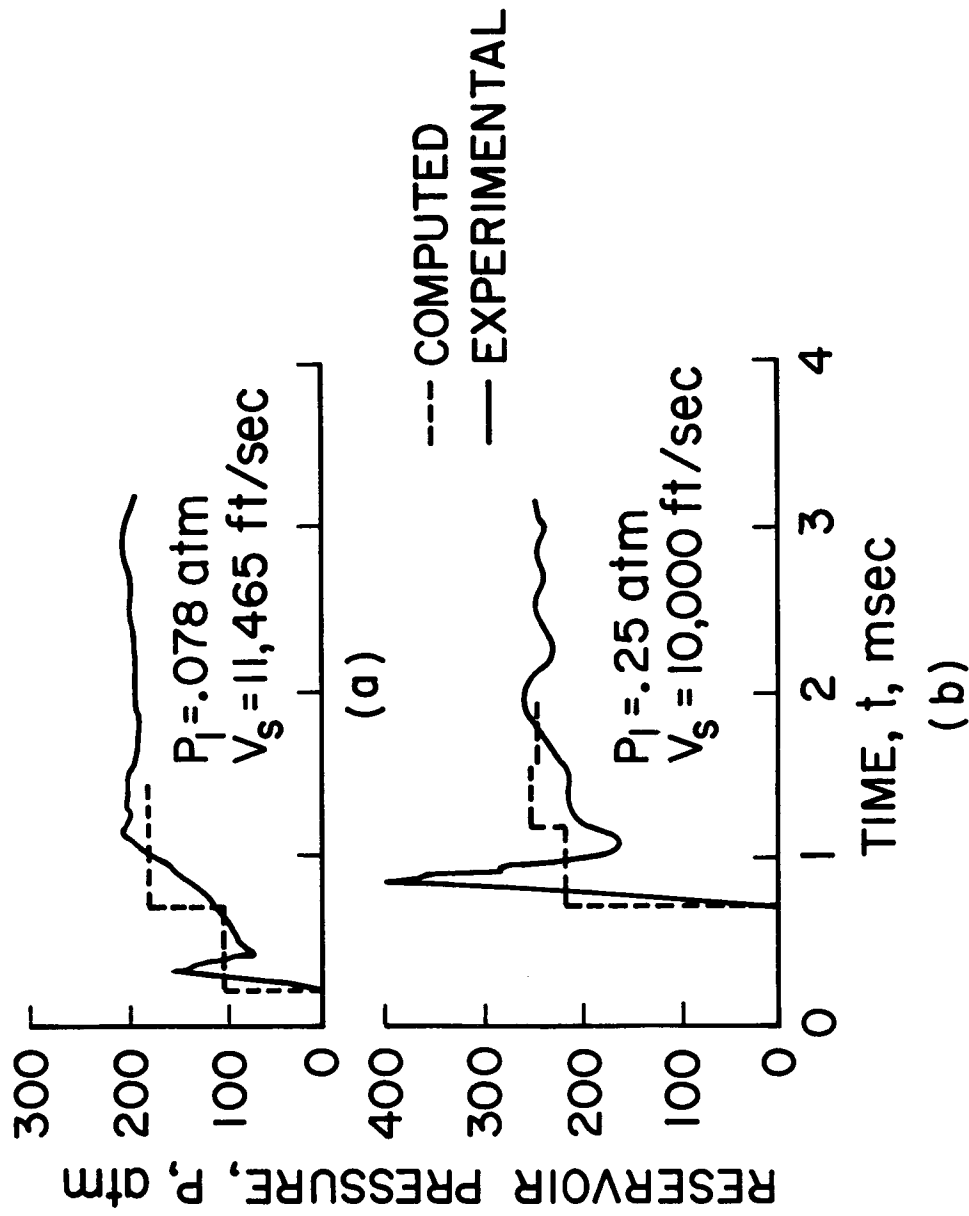Figure 8.- Pressure histories in reservoir of driven tube; $P_1 = 0.25$ atm.

Figure 9.- Effect of initial driven tube pressure on early reservoir pressure histories (sonic orifice-driven tube area ratio = 0.718).

Figure 10.- Duration of steady flow in the shock tunnel nozzle.
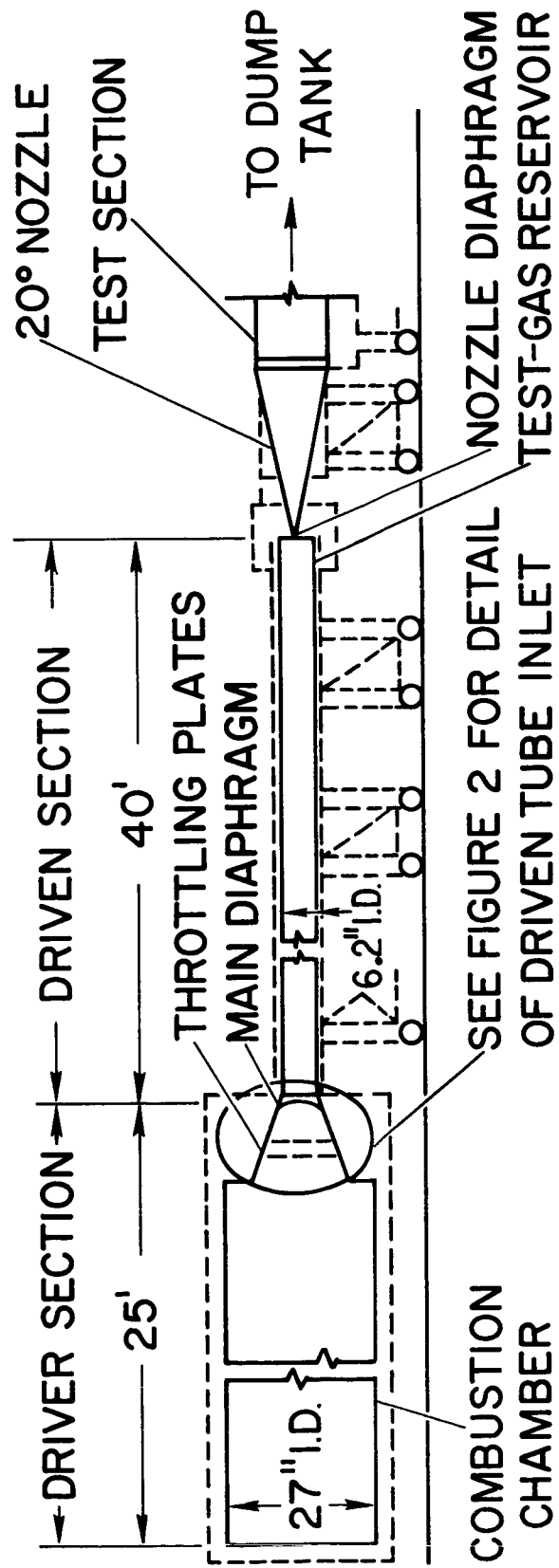
Figure 1.- Schematic drawing of Ames 1-foot shock tunnel.
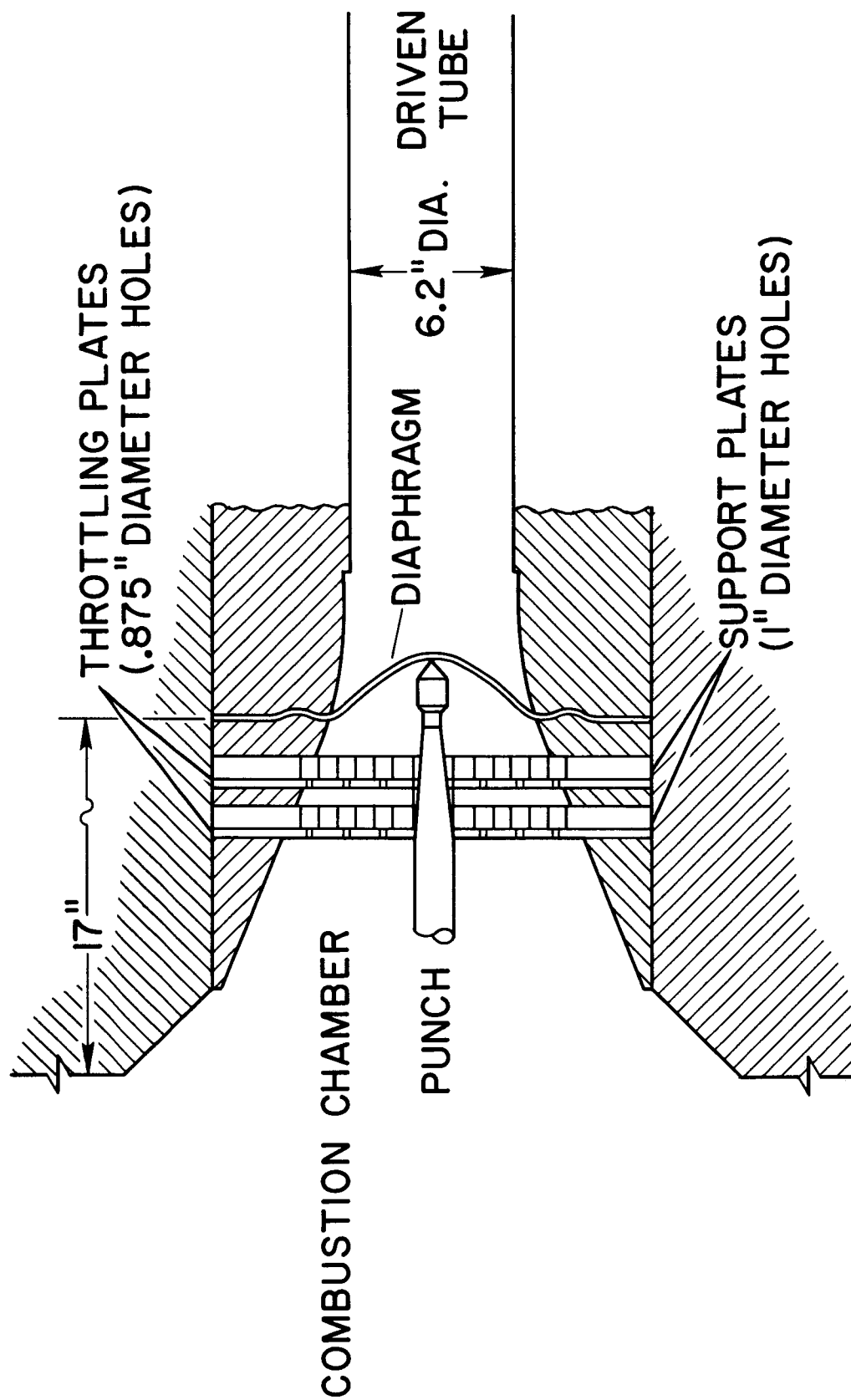
Figure 2.- Detail of driven tube inlet showing throttling plates and diaphragm arrangement.
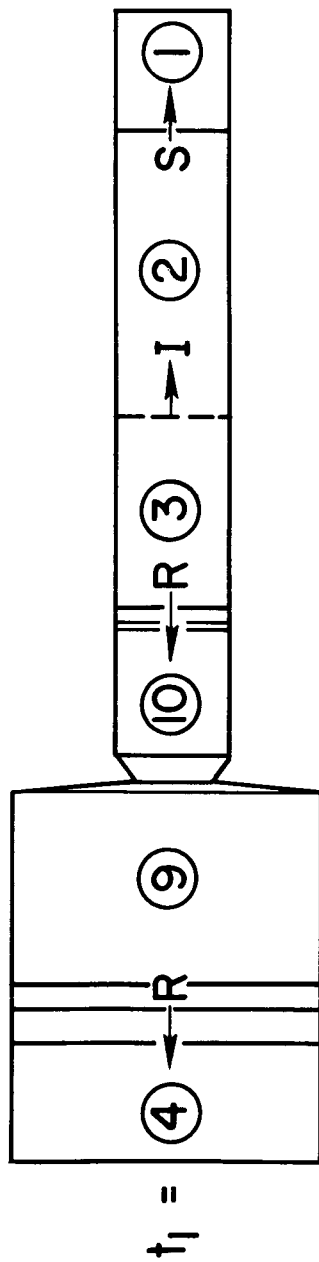
(a) PHYSICAL LOCATION OF PRESSURE WAVES AT A TIME t_1
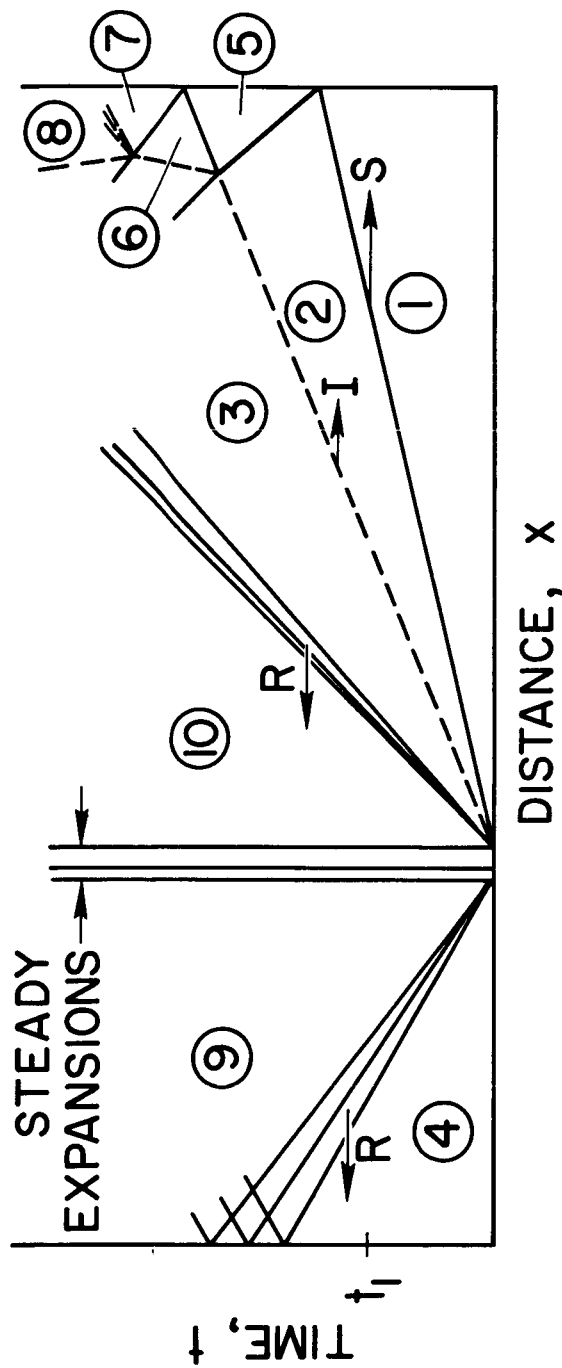
(b) DISTANCE HISTORY OF UNSTEADY PRESSURE WAVES

Figure 3.— Wave model used by first computer program.

Figure 4.- Facility operating lines.

Figure 5.- Wave diagram for the driven tube; $P_1 = 0.25$ atm, no throttling plates.

Figure 6.- Comparison between theoretical and experimental pressures obtained at a station 5 feet downstream of the diaphragm.

Figure 7.- Long-time reservoir pressure-history for various driven tube loadings.

Figure 8.- Pressure histories in reservoir of driven tube; P = 0.25 atm.

Figure 9.- Effect of initial driven tube pressure on early reservoir pressure histories (sonic orifice-driven tube area ratio = 0.718).
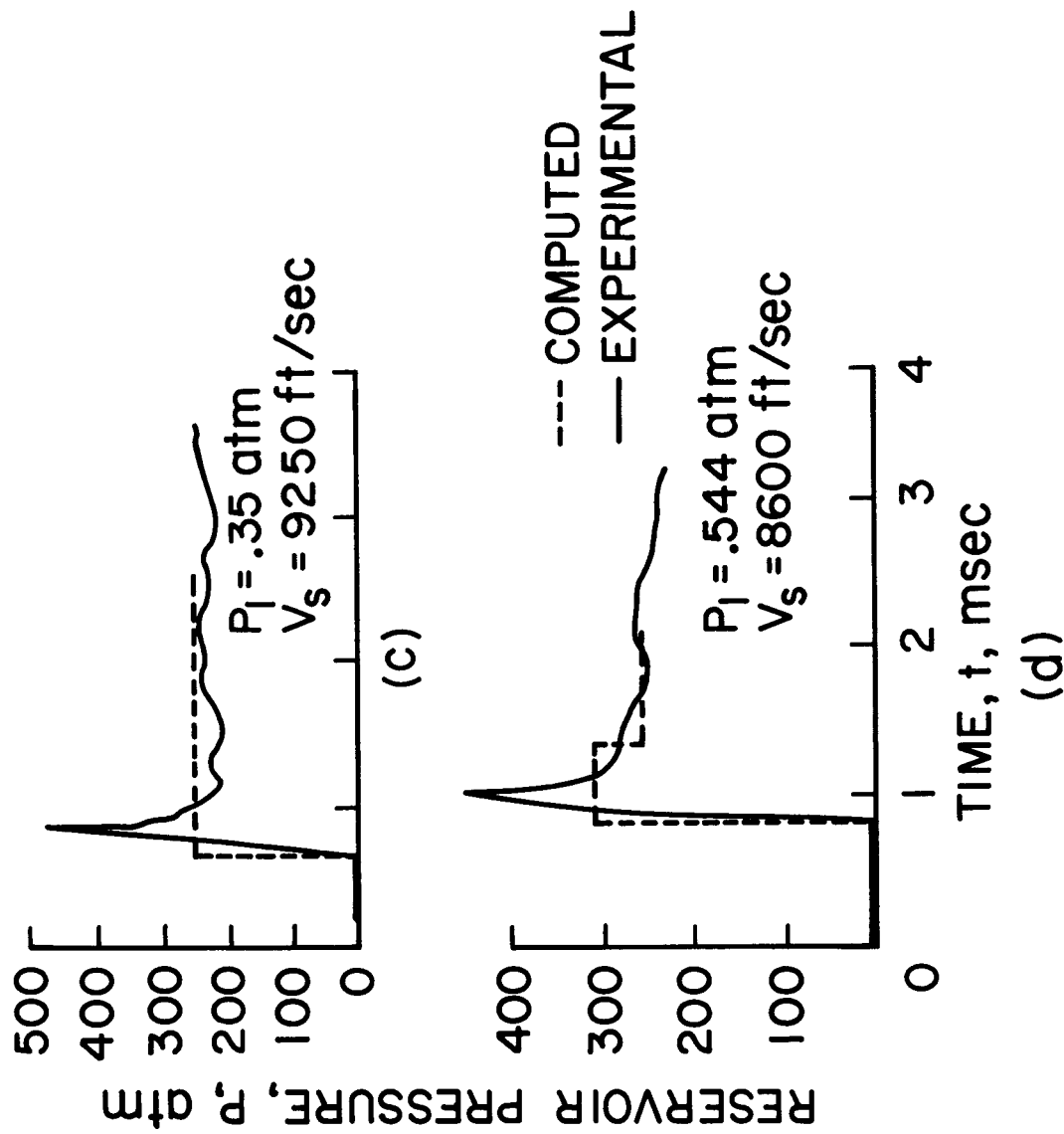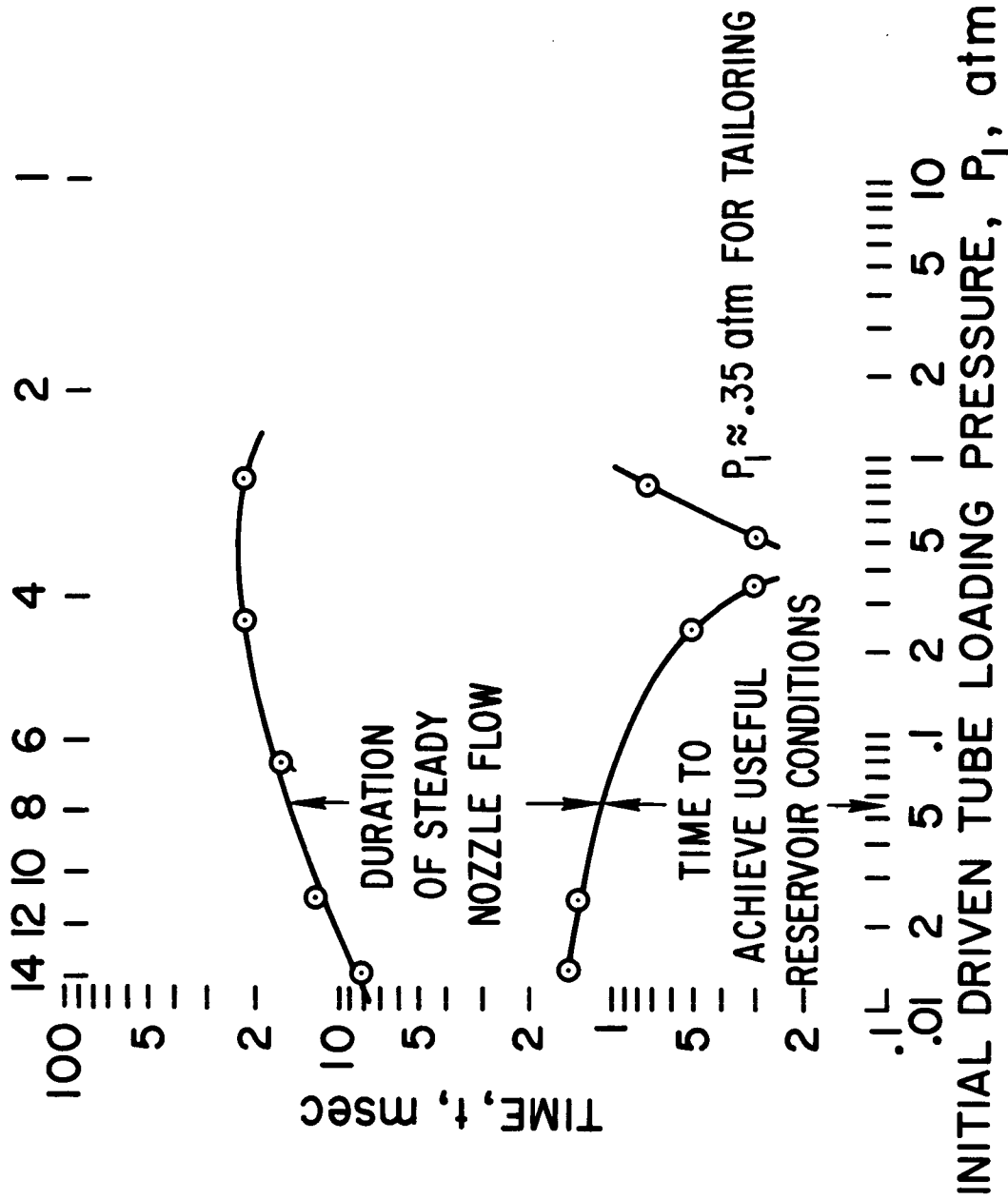
Figure 9.- Concluded.

Figure 10.- Duration of steady flow in the shock tunnel nozzle.